STUDY OF DEFORMATION EFFECTS ON FUSION PROBABILITIES WITH SKYRME INTERACTION AND OTHER PROXIMITY BASED POTENTIALS*

Raj Kumari†, Lavneet Kaur

Department of Physics, Panjab University, Chandigarh 160 014, India

(Received October 30, 2013)

The Skyrme energy density formalism (SEDF) is used to study the effect of deformation on the fusion barriers and fusion cross-sections. Proximity based potentials like AW 95, Bass 80 and Denisov DP are also used for a comparative analysis. In this paper, deformation enters via deformed Coulomb potential between the two colliding nuclei. Our detailed study reveals that the deformed Coulomb potential alone can affect interaction potential significantly in the inner region as well as fusion probabilities at below barrier energies.

DOI:10.5506/APhysPolB.45.391
PACS numbers: 24.10.–i, 25.60.Pj, 25.70.Jj

1. Introduction

The study of heavy-ion collisions gives us a possibility to examine nuclear interactions in the form of ion–ion potential as well as fusion [1] at low incident energies and in the form of multi-fragmentation [2], nuclear flow [3] *etc.* at intermediate incident energies. The shape of the nuclei participating in a reaction affects the barrier height, which is of great significance for sub-barrier fusion reactions. A number of studies have been carried out in the recent past on the role of deformation in the sub-barrier fusion cross-section using quantum diffusion approach [4]. At low incident energies, many potentials are available to calculate the nuclear part of the interaction potential like proximity based potential models [1, 5]. As far as Coulomb part of the interaction potential is concerned, a very few efforts have been made to modify it [6]. So in the present study, only Coulomb deformation effects are taken into account.

* Presented at the XXXIII Mazurian Lakes Conference on Physics, Piaski, Poland, September 1–7, 2013.

† rajkumari80pu@gmail.com; rajruhi06@gmail.com

2. Methodology

The total interaction potential $V_{\mathrm{T}}(R)$ can be calculated using the relation [1–5]

$$V_{\mathrm{T}}(R) = V_{\mathrm{N}}(R) + V_{\mathrm{C}}(R)\,, \tag{1}$$

here, $V_{\mathrm{N}}(R)$ is the nuclear part and $V_{\mathrm{C}}(R)$ is the Coulomb part of total interaction potential.

2.1. Nuclear potential

We have employed two models to calculate the nuclear potentials.

2.1.1. Skyrme energy density formalism

In this model, the nuclear part of the interaction potential $V_{\mathrm{N}}(R)$ is defined as the difference between the energy expectation value E of two colliding nuclei at a finite distance R and at infinity [5]

$$V_{\mathrm{N}}(R) = E(R) - E(\infty)\,. \tag{2}$$

The energy E at infinity represents the binding energy of a nucleus in isolation. The energy expectation value E is given by

$$E = \int H(\vec{r})d\vec{r}. \tag{3}$$

The energy density function H is a function of nucleonic density ρ, kinetic energy density τ and spin density $\vec{J}$. The nuclear potential $V_{\mathrm{N}}(R)$ is the sum of spin-independent part $V_P(R)$ and spin-dependent part $V_J(R)$

$$V_{\mathrm{N}}(R) = V_P(R) + V_J(R)\,. \tag{4}$$

2.1.2. Proximity potential

The interaction potential $V_{\mathrm{N}}(R)$ between two colliding surfaces therefore, is given by [1]

$$V_{\mathrm{N}} = 4\pi\gamma b\overline{C}\Phi\left(\frac{R - C_1 - C_2}{b}\right)\ \mathrm{MeV}\,, \tag{5}$$

where, $\overline{C}$ $(= (C_1C_2)/(C_1 + C_2\ ))$, b and R are the reduced radius, surface width and central separation, respectively. Here, C is the central radius and Φ is the universal nuclear function [7]. The surface energy coefficient γ has the form

$$\gamma = \gamma_0\left[1 - k_{\mathrm{s}}\left(\frac{N-Z}{A}\right)^2\right]. \tag{6}$$

Here, γ_0 and k_s are the surface energy coefficient and surface asymmetry constant, respectively. The details on AW 95, Bass 80 and Denisov DP potentials can be found in Ref. [1].

2.2. Deformed Coulomb potential

The expression for the Coulomb interaction $V_C(R,\theta)$ between two deformed colliding nuclei is given by Ref. [8]

$$V_C(R,\theta) = \frac{Z_1 Z_2 e^2}{R} + \sqrt{\frac{9}{20\pi}}\frac{Z_1 Z_2 e^2}{R^3}\sum_{i=1}^{2} R_i^2 \beta_{2i} P_2(\cos\theta_i) + \frac{3}{7\pi}\frac{Z_1 Z_2 e^2}{R^3}\sum_{i=1}^{2} R_i^2 [(\beta_{2i} P_2(\cos\theta_i)]^2 , \quad (7)$$

where θ_i is the angle between the radius vector $\vec{R}$ and the symmetry axis of the i^{th} nucleus and R_i being the effective sharp radius of ith nucleus. The values of quadrupole deformation parameter (β_{2i}) for the present study are borrowed from Ref. [9]. As the colliding nuclei may have many possible orientations (θ_1, θ_2) during the experiment, we have taken average over all possible relative orientations of two deformed colliding nuclei while studying the fusion between them. Once total interaction potential $V_T(R)$ is calculated, the barrier height V_B, barrier position R_B and fusion cross-section can be calculated using the methods mentioned in Ref. [1].

3. Results and discussions

We have calculated the fusion barriers and fusion probabilities for the reactions of ^{58}Ni+^{74}Ge, ^{40}Ca+^{96}Zr, ^{64}Ni+^{74}Ge and ^{16}O+^{76}Ge. Depending upon the shapes of the projectile–target, these reactions are grouped under different categories: spherical–oblate (S+O), spherical–prolate (S+P), oblate–oblate (O+O) and prolate–prolate (P+P).

In Fig. 1, we display the total interaction potential V_T [MeV] as a function of internuclear distance R [fm] for the reactions of ^{58}Ni+^{74}Ge and ^{40}Ca+^{96}Zr. In the figure, grey lines correspond to the total interaction potential calculated by assuming the colliding nuclei to be spherical (*i.e.* $\beta_{21} = \beta_{22} = 0$). On the other hand, black lines represent the total interaction potential calculated by taking into consideration the deformation of the colliding nuclei.

Now in Fig. 1, the projectile (^{58}Ni) is spherical and target (^{74}Ge) is oblate deformed, whereas, the projectile (^{40}Ca) is spherical and the target (^{96}Zr) is prolate deformed. Both SEDF as well as proximity based potentials

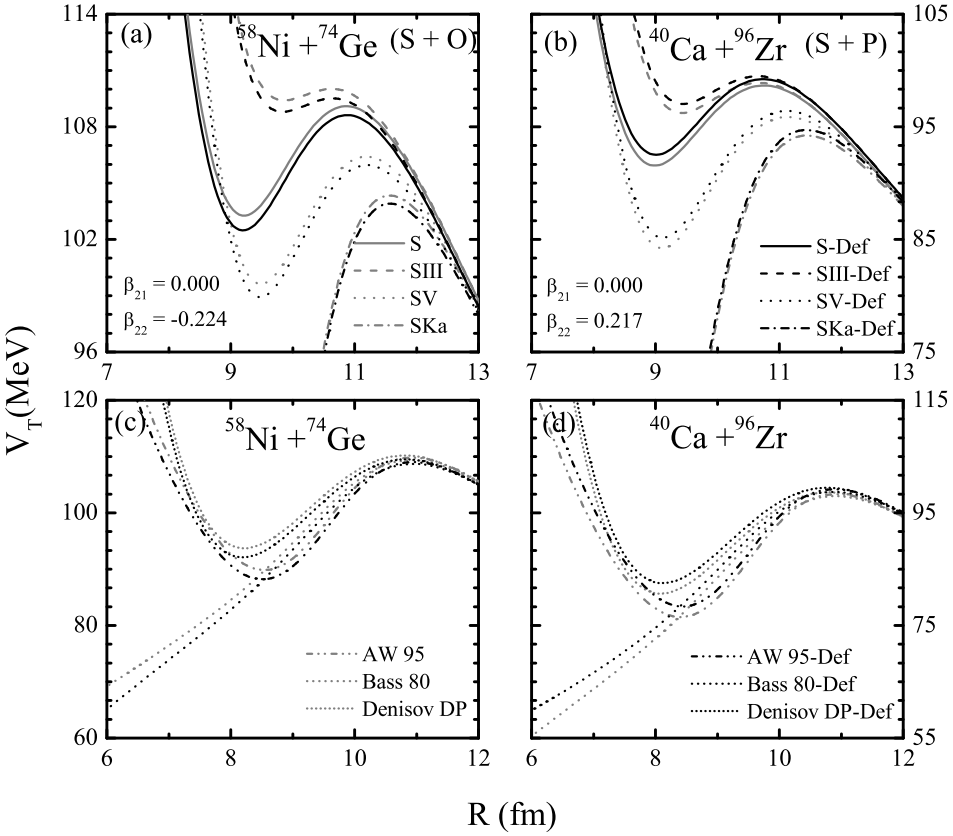

Fig. 1. Total interaction potential V_{T} [MeV] as a function of internuclear distance R [fm] for the reactions of ^{58}Ni+^{74}Ge and ^{40}Ca+^{96}Zr. The upper panels (a) and (b) display the calculations of SEDF (using different Skyrme forces) and the lower panels (c) and (d) display the calculations corresponding to AW 95, Bass 80 and Denisov DP. Various lines are explained in the text.

results in similar trends. From Fig. 1, we observed that the total interaction potential in the inner region gets modified by adding deformation to the Coulomb potential. It is noticed that the depth of the fusion pocket for the fusion of S+O colliding nuclei is more than for the (spherical–spherical) S+S reaction. Similar trend is also observed for the reaction of O+O (^{64}Ni+^{74}Ge and ^{28}Si+^{62}Ni). These reactions are not displayed here. Whereas, the fusion pocket becomes shallower for the fusion of S+P reaction compared to the S+S reaction. This trend is also observed for P+P (^{16}O+^{76}Ge and ^{16}O+^{92}Zr) reactions. These reactions are not shown here.

In Fig. 2, we display the fusion cross-section $\sigma_{\rm fus}$ [mb] as a function of center-of-mass energy $E_{\rm cm}$ [MeV]. Various lines have the same meaning as in Fig. 1. In Fig. 2, we noticed that there is a slight increase in the fusion probability for S+O (^{58}Ni+^{74}Ge) reaction compared to the S+S case at sub-barrier energies. Similar trend is also observed for the reaction of O+O (^{64}Ni+^{74}Ge). However, we observe that there is a decrease in the fusion probability for S+P (^{40}Ca+^{96}Zr) reaction than for the S+S reaction. Similar trend is noticed in P+P (^{16}O+^{76}Ge). The reaction of O+O (^{64}Ni+^{74}Ge) and P+P (^{16}O+^{76}Ge) are not displayed here. One clearly observes that there is an increase in the fusion probabilities for spherical–oblate and oblate–oblate deformed nuclei and decrease for the spherical–oblate and oblate–oblate deformed nuclei compared to the spherical–spherical case at sub-barrier energies.

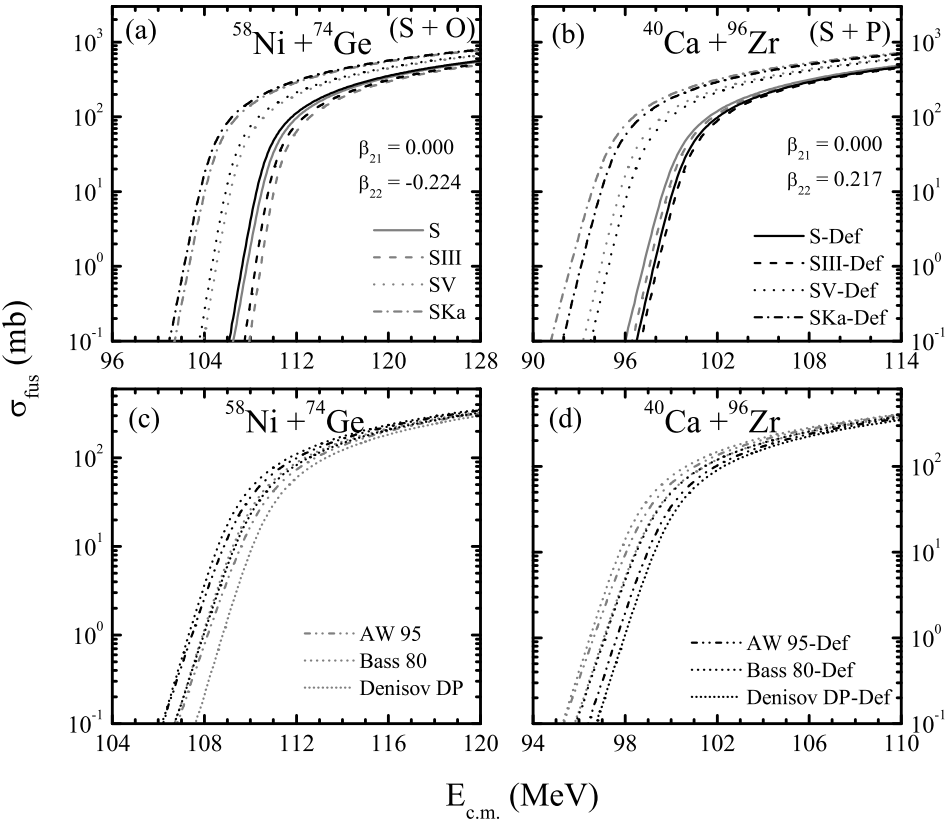

Fig. 2. The fusion cross-section $\sigma_{\rm fus}$ [mb] as a function of centre-of-mass energy $E_{\rm cm}$ [MeV] for the reactions of ^{58}Ni+^{74}Ge and ^{40}Ca+^{96}Zr. Various lines have the same meaning as in Fig. 1.

4. Summary

In this paper, we studied the role of the deformed Coulomb potential on fusion probabilities using the Skyrme energy density formalism and other proximity based potentials such as AW 95, Bass 80 and Denisov DP. We found that the fusion probabilities at sub-barrier energies differ for deformed colliding nuclei compared to spherical colliding nuclei and these differences are observed to be smaller compared to differences due to different choices of nuclear potential for these selected reactions. A study of other reactions of heavily deformed nuclei, where we have observed that this difference increases with increase in the value of quadrupole deformation parameter, is still under progress. Hence, the fusion probabilities at below barrier energies has a strong dependence on the shape of the colliding nuclei.

R.K. gratefully acknowledges the research grant No. 09/135(0635)/2011-EMR-I from the Council of Scientific and Industrial Research (CSIR), New Delhi. The authors are thankful to Professor Rajeev K. Puri for valuable suggestions and fruitful discussions on the present work.

REFERENCES

[1] I. Dutt, R.K. Puri, *Phys. Rev.* **C81**, 044615 (2010); **C81**, 047601 (2010); **C81**, 064608 (2010); **C81**, 064609 (2010); R. Kumari, *Nucl. Phys.* **A917**, 85 (2013) and references therein.

[2] Y.K. Vermani *et al.*, *J. Phys. G: Nucl. Part. Phys.* **37**, 015105 (2010); S. Goyal, R.K. Puri, *Phys. Rev.* **C83**, 047601 (2011); S. Kaur, R.K. Puri, *Phys. Rev.* **C87**, 014620 (2013).

[3] S. Gautam *et al.*, *Phys. Rev.* **C83**, 014603 (2011); **C83**, 034606 (2011); **C85**, 067601 (2012); **C86**, 034607 (2012); R. Bansal *et al.*, *Phys. Rev.* **C87**, 061602 (2013).

[4] V.V. Sargsyan *et al.*, *Phys. Rev.* **C84**, 064614 (2011); **C85**, 017603 (2012); **C85**, 037602 (2012).

[5] R.K. Puri, R.K. Gupta, *J. Phys. G: Nucl. Part. Phys.* **17**, 1933 (1991); **18**, 903 (1992); *Phys. Rev.* **C45**, 1837 (1992); **C43**, 315 (1991); M.K. Sharma *et al.*, *Eur. Phys. J.* **A2**, 69 (1998); R.K. Puri, N.K. Dhiman, *Eur. Phys. J.* **A23**, 429 (2005).

[6] C.K. Phookan, K. Kalita, *Nucl. Phys.* **A899**, 29 (2013).

[7] J. Blocki, J. Randrup, W.J. Swiatecki, C.F. Tsang, *Ann. Phys.* **105**, 427 (1977).

[8] V.Yu. Denisov, N.A. Pilipenko, *Phys. Rev.* **C76**, 014602 (2007); *Ukr. J. Phys.* **53**, 845 (2008); *Phys. At. Nucl.* **73**, 1152 (2010).

[9] P. Moller *et al.*, *At. Data Nucl. Data Tables* **59**, 185 (1995).